The Astrophysical Journal, 623:1000–1010, 2005 April 20

EFFECTS OF ROTATION ON THE REVIVAL OF A STALLED SHOCK IN SUPERNOVA EXPLOSIONS

Tatsuya Yamasaki[1] and Shoichi Yamada[2,3]
Received 2004 November 11; accepted 2004 December 31

ABSTRACT

In order to infer the effects of rotation on the revival of a stalled shock in supernova explosions, we investigate steady accretion flows with a standing shock. We first obtain a series of solutions for equations describing nonrotating, spherically symmetric flows and confirm the results of preceding papers, that for a given mass accretion rate, there is a critical luminosity of irradiating neutrinos above which there exists no steady solution. Below the critical value, we find two branches of solutions; one is stable and the other is unstable against radial perturbations. With a simple argument based on the Riemann problem, we can identify the critical luminosity as that at which the stalled shock revives. We also obtain a condition satisfied by the flow velocity for the critical luminosity, which can easily be applied to the rotational case. If a collapsing star rotates, the accretion flow is nonspherical as a consequence of centrifugal forces. Flows are accelerated near the rotation axis, whereas they are decelerated near the equatorial plane. As a result, the critical luminosity is lowered; that is, rotation assists the revival of a stalled shock. According to our calculations, the critical luminosity is ~25% lower for a mass accretion rate of 1 $M_{\odot}$ s^{-1} and a rotational frequency of 0.1 Hz at a radius of 1000 km than that for a spherically symmetric flow with the same mass accretion rate. We find that the condition on the flow velocity at the critical luminosity is first satisfied at the rotation axis. This suggests that shock revival is triggered on the rotation axis and a jetlike explosion ensues.

Subject headings: hydrodynamics — shock waves — stars: rotation — supernovae: general

1. INTRODUCTION

Core-collapse supernovae play important roles in, for example, star formation, the evolution of galaxies and the entire universe, and the acceleration of cosmic-ray particles, owing to their nucleosynthesis, energetic shock waves, and high luminosity. Recently, the phenomenon has been put in the spotlight because of a likely association with gamma-ray bursts. Unfortunately, however, the mechanism behind supernova explosions is still unresolved (see, e.g., Wheeler 2003 for a review).

Supernova explosions commence with the gravitational collapse of massive stars at the ends of their lives. When the nuclear saturation density is reached at the center of the core, the core bounce occurs, producing a shock wave that starts to propagate outward in the core. There is near-consensus among researchers that this shock wave does not produce the supernova explosion directly, since the shock loses energy by photodissociation of nuclei, as well as by neutrino cooling, and stalls somewhere inside the core. It is widely expected that the shock will be revived by irradiation from neutrinos diffusing out of the proto–neutron star, the scenario originally proposed by Wilson (1985). Although many researchers have studied this scenario intensively and extensively, state-of-the-art numerical simulations so far have shown that as long as the collapse is spherically symmetric, the stalled shocks do not revive (Liebendörfer et al. 2001; Buras et al. 2003; Thompson et al. 2003; Liebendörfer et al. 2005).

These simulations are concerned with the dynamical evolution of the entire core from the onset of the collapse till long after the stagnation of the shock. Burrows & Goshy (1993) took a contrary approach, focusing on the revival of the stalled shock wave. After the shock stagnates because of the energy losses mentioned above, the accretion flows through the standing shock wave are quasi-steady (see Janka 2001 for a criticism on this point). Burrows & Goshy approximated these flows with steady state solutions for constant mass accretion rates and neutrino luminosities. Varying these constant values, they found that for a given mass accretion rate there is a critical neutrino luminosity above which there exist no steady solutions. Using this fact, they argued that the revival of the stalled shock occurs when the neutrino luminosity exceeds this critical value. The existence of the critical luminosity was also observed in numerical experiments done by Janka & Müller (1996), in which they artificially increased neutrino luminosities in their failed-explosion models and saw what happened to the stalled shocks. Merits of these steady state calculations are that not only are they relatively simple computationally, but they can also clearly demonstrate, if only qualitatively, the cause of the failure to produce explosions—that is, according to this theory, an inappropriate combination of the neutrino luminosity and the mass accretion rate.

So far, we have been talking about studies of spherically symmetric collapse. However, several observations suggest that supernova explosions are intrinsically asymmetric. For example, Leonard et al. (2000) and Wang et al. (2002) have observed linear polarizations of a few percent for photons from collapse-driven supernovae and argued that the stellar envelopes are globally asymmetric, either oblate or prolate, with an aspect ratio of ~2. We also know that supernova remnants are asymmetric in general. One can easily imagine a couple of possible causes for this asymmetry, for example, hydrodynamic instabilities, rotation, and magnetic fields. In fact, young pulsars are thought to have rather large angular momenta (Kaspi et al. 1994; van der Swaluw & Wu 2001) and magnetic fields (Kulkarni

[1] Department of Astronomy, Faculty of Science, Kyoto University, Oiwake-cho, Sakyo-ku, Kyoto 606-8502, Japan; yamasaki@kusastro.kyoto-u.ac.jp.
[2] School of Science and Engineering, Waseda University, 3-4-1 Okubo, Shinjuku-ku, Tokyo 169-8555, Japan; shoichi@heap.phys.waseda.ac.jp.
[3] Advanced Research Institute for Science and Engineering, Waseda University, 3-4-1 Okubo, Shinjuku-ku, Tokyo 169-8555, Japan.

1992), which are probably inherited from the precollapse stars. It is also believed that some convective motions occur in the supernova core. Large-scale nonspherical oscillations of the standing accretion shocks may also cause the stellar envelope to be globally asymmetric (Blondin et al. 2003).

Among these effects, we pay particular attention to stellar rotation in this paper. Note, however, that the rotation of the core may not be so rapid after all. Recent evolution models by Heger et al. (2000, 2004) suggest that the transport of angular momentum during the quasi-static evolutionary phase of the progenitor deprives the core of a substantial fraction of its angular momentum, particularly when magnetic torque is taken into account (Spruit 2002; Heger et al. 2004). If this is really the case, rotation will play no significant role in the dynamics of core collapse, as shown by Buras et al. (2003; see also Müller et al. 2004). One should bear in mind, however, that these evolution models are based on one-dimensional calculations and have some uncertainties in the mechanism and treatment of angular momentum transport.

The dynamics of rotational collapse has been explored numerically by some authors. For example, Mönchmeyer & Müller (1989) and Yamada & Sato (1994) demonstrated that rapid rotation tends to weaken the prompt shock wave because the centrifugal force prevents the core from contracting sufficiently. Fryer & Heger (2000) found that the efficiency of energy transfer by convection was reduced by the decrease of effective gravity near the equatorial plane due to the centrifugal force, and as a result, the shock does not propagate as much as in the no-rotation case. They also asserted that the resultant anisotropy of energy transfer would have made the explosion jetlike had it been successful. Kotake et al. (2003) estimated the anisotropy of neutrino radiation due to a rotating core. They claimed that the deformed neutrinosphere, which is in general oblate, yields a neutrino flux and a heating rate that are larger near the rotation axis than near the equatorial plane. Given this result by Kotake et al. (2003) and the results by Shimizu et al. (2001) that such anisotropic neutrino irradiation could lead to a successful jetlike explosion, we may well expect rotation to help along the explosion in the neutrino-heating scenario.

In order to see the effects of rotation more clearly, if qualitatively, we follow the lead of Burrows & Goshy (1993). We solve the time-independent Euler equations describing steady accretion flows through a standing shock, taking rotation into account. We pay particular attention to how the critical luminosity of neutrinos is altered by stellar rotation and demonstrate that rotation assists the revival of the stalled shock.

This paper is organized as follows: In the next section, we discuss the spherically symmetric case. We find two branches of steady solutions and discuss the revival of the shock wave, employing the critical luminosity. We examine in § 3 the stability of the two solution branches obtained in § 2. In § 4, we analyze the steady axisymmetric solutions with rotation and discuss the effect of rotation on the revival of the stalled shock. The final section is devoted to a summary and some additional discussion.

2. SPHERICALLY SYMMETRIC FLOWS WITH A STANDING SHOCK

In this and the next section, we discuss spherically symmetric flows, solving one-dimensional hydrodynamic equations. The calculations in this section are similar to those of Burrows & Goshy (1993). After the shock stalls, the mass accretion rate and neutrino luminosities change rather slowly, and the flows become quasi-steady. Idealizing this situation, in this section we seek steady solutions for the accretion flow.

Since our purpose in this paper is not to quantitatively determine the critical luminosity of neutrinos, we make the following assumptions and simplifications:

1. We do not consider the flows outside the shock wave in detail, simply assuming a free fall, and restrict our calculations to the inside of the shock surface.
2. Newtonian formulations are adopted, because the region of interest is outside the neutron star and general relativistic effects are negligible there.
3. We do not solve the neutrino transfer equations, assuming that the luminosity and energy of the neutrinos are independent of radius. It is also assumed that the neutrinos are thermal with a fixed temperature ($T_\nu = 4.5$ MeV), for simplicity.
4. A simplified equation of state and rates of neutrino heating and cooling are employed.
5. Photodissociation of nuclei, magnetic fields, and convection are neglected for simplicity, although there should exist regions where the flows are convectively unstable.

Then, the basic equations describing steady, spherically symmetric accretion flows are given in spherical coordinates by

$$4\pi r^2 \rho u_r = \dot{M}, \tag{1}$$

$$u_r \frac{du_r}{dr} + \frac{1}{\rho}\frac{dp}{dr} + \frac{GM}{r^2} = 0, \qquad u_r \frac{d\epsilon}{dr} - \frac{p}{\rho^2} u_r \frac{d\rho}{dr} = \dot{q}, \tag{2}$$

where u_r, ρ, p, and ϵ denote the radial velocity, density, pressure, and specific internal energy, respectively; $\dot{M}$, G, M, and $\dot{q}$ are the mass accretion rate, gravitational constant, neutron star mass, and net heating rate due to neutrino irradiation, respectively. For the neutron star's mass, we adopt 1.3 $M_\odot$.

The pressure and specific internal energy of nucleons, photons, and relativistic particles are approximately written as

$$p = \frac{11\pi^2}{180}\frac{k^4}{c^3\hbar^3}T^4 + \frac{\rho k T}{m_N}, \qquad \epsilon = \frac{11\pi^2}{60}\frac{k^4}{c^3\hbar^3}\frac{T^4}{\rho} + \frac{3}{2}\frac{kT}{m_N}, \tag{3}$$

where k, c, $\hbar$, and m_N are the Boltzmann constant, speed of light, Planck constant, and nucleon mass, respectively; T is the temperature of matter and photons.

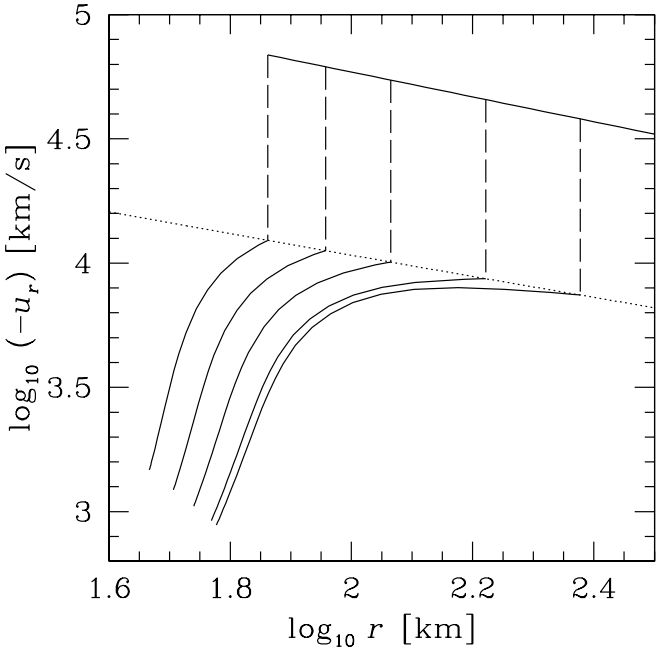

FIG. 1*a*

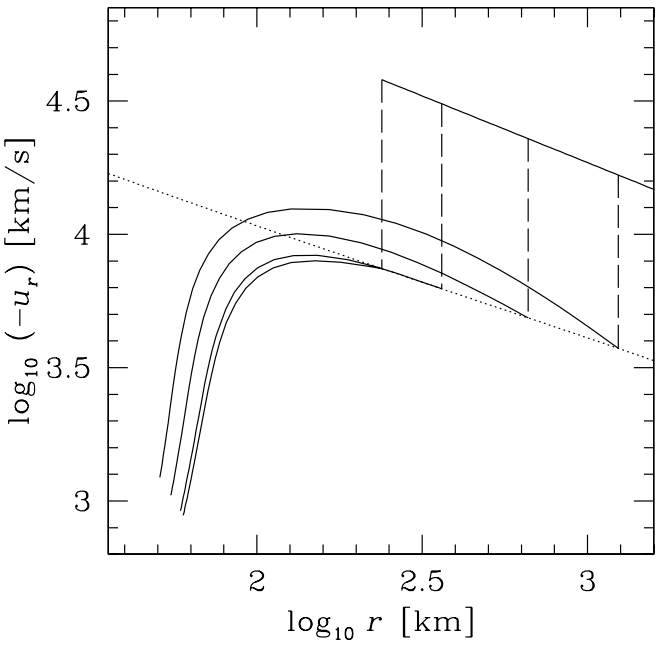

FIG. 1*b*

FIG. 1.—(*a*) Inner solution curves for spherical steady accretion flows with $\dot{M} = 2.0\,M_\odot\ \mathrm{s}^{-1}$ and $L_{\nu_e} = (5, 6, 7, 8) \times 10^{52}$ and 8.3167×10^{52} ergs s^{-1} (the critical value), from left to right. (*b*) Outer solution curves for steady accretion flows with $\dot{M} = 2.0\,M_\odot\ \mathrm{s}^{-1}$ and $L_{\nu_e} = (6, 7, 8) \times 10^{52}$ and 8.3167×10^{52} ergs s^{-1}, from left to right. Dashed lines denote shock jumps. Dotted lines show the downstream values satisfying the Rankine-Hugoniot relations at each radius.

As for the heating and cooling processes, we take into account only the absorption and emission of neutrinos by nucleons. We adopt the formulae given by Herant et al. (1992) for degeneracy factor $\eta = 0$; that is,

$$\dot{q} = 4.8 \times 10^{32} \left[1 - \sqrt{1 - (r_\nu/r)^2}\right] \frac{L_{\nu_e}(\mathrm{foe\ s^{-1}})}{2\pi r_\nu^2} T_\nu^2 - 2.0 \times 10^{18} T^6 \quad (\mathrm{ergs\ s^{-1}\ g^{-1}}), \tag{4}$$

where L_{ν_e} is the luminosity of electron neutrinos (1 foe = 10^{51} ergs), which is assumed to be equal to that of antielectron neutrinos, and r_ν is the radius of the neutrinosphere, that is, the inner boundary.

The outer and inner boundaries of the calculations are set at the shock surface and the neutrinosphere, respectively. We impose the Rankine-Hugoniot relations at the shock surface. The flow into the shock is assumed to be a free fall with velocity $u_f = -(2GM/r)^{1/2}$ and temperature of zero. Thus, the outer boundary conditions are written as

$$\rho u_r^2 + p = \rho_f u_f^2, \qquad \tfrac{1}{2} u_r^2 + \epsilon + p/\rho = \tfrac{1}{2} u_f^2, \tag{5}$$

where ρ_f is the upstream density at the shock surface. The continuity equation is automatically satisfied by imposing equation (1) on each side of the shock. We impose the condition that the density is 10^{11} g cm^{-3} at the inner boundary; this approximately corresponds to the condition that the optical depth from the neutrinosphere to infinity is equal to $\frac{2}{3}$. The latter condition was adopted by Burrows & Goshy (1993).

We note that the position of the inner boundary is determined by the relation

$$L_{\nu_e} = \left(7\sigma T_\nu^4/16\right)\left(4\pi r_\nu^2\right), \tag{6}$$

where σ is the Stefan-Boltzmann constant. On the other hand, the position of the outer boundary is determined so as to satisfy the above jump conditions. Thus, the problem can be regarded as an eigenvalue problem. We solve these equations for a wide range of values of the mass accretion rate and the neutrino luminosity.

The results of the calculations are shown in Figures 1 and 2. In Figure 1, one can see there are two solutions for a given mass accretion rate and neutrino luminosity when the neutrino luminosity is below a certain critical value. The shock radii of these two solutions differ. From here on, we refer to the solution with the smaller shock radius as the inner solution and to the other solution as the outer solution. As shown in Figure 2, as the neutrino luminosity is raised with the mass accretion rate fixed, the shock radius for the inner solution becomes larger, whereas that for the outer solution becomes smaller. The two solutions coincide when the luminosity reaches the critical value. For luminosities above the critical value, there is no solution. (This critical value of the neutrino luminosity is shown in Fig. 8 below.) Note that when the luminosity is close to the critical value, the shock radii are insensitive to the luminosity. Although our formulation is different in detail from that of Burrows & Goshy, the results are in good agreement (cf. Fig. 1 of Burrows & Goshy 1993). As mentioned, the shock radius for the critical luminosity is almost independent of the mass accretion rate; it is about 200–300 km according to our calculations.

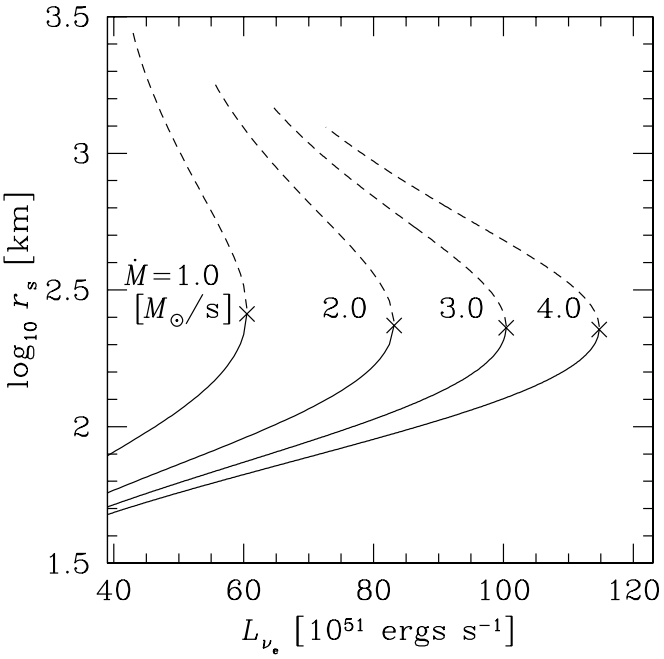

FIG. 2.—Radius of the shock surface for the inner (*solid curves*) and outer (*dashed curves*) solutions, with $\dot{M}$ = 1.0, 2.0, 3.0, and 4.0 $M_\odot$ s^{-1} from left to right. Crosses represent the critical points.

This behavior of the solutions can be understood if one recalls the adiabatic subsonic Bondi-Hoyle flow (see Shapiro & Teukolsky 1983). Here we introduce $u_{\rm post}(r)$ as the postshock velocity that we would obtain if the shock radius were r. The velocity $u_{\rm post}(r)$ is shown by dotted lines in Figure 1. The subsonic adiabatic flows accelerate outside a certain radius, whereas they decelerate inside that radius. The critical radius is determined by the balance of gravitational energy and thermal energy and is close to the sonic point in a transonic accretion flow. On the other hand, the free-fall velocity decreases monotonically. Furthermore, the acceleration of the adiabatic flow is larger than that of the free fall outside the critical radius, owing to the pressure gradient force. Therefore, if any, there are two radii where the accretion flow joins with the free-falling stream via the Rankine-Hugoniot relations. In other words, the solution curve of the adiabatic accretion flow $u_r(r)$ intersects $u_{\rm post}(r)$ at two points. Although the solution curves are somewhat modified if one takes account of the neutrino irradiation, this behavior is not altered for the amplitudes of neutrino luminosity under consideration. The irradiation tends to heat and push out the infalling matter. Hence, as the luminosity gets larger, the infall velocity gets smaller in the whole range and the solution curves go down. When the luminosity exceeds a critical value, there exists no point where the subsonic accretion flow joins with the free-falling stream, via the Rankine-Hugoniot relations: the solution curves of the accretion flow $u_r(r)$ never intersect $u_{\rm post}(r)$.

From the above explanation, we can also understand another important property of the solutions. As the luminosity is raised with the mass accretion rate fixed, the radial derivative of the velocity of the accretion flow at the shock radius, $du_r(r)/dr$, becomes larger for the inner solutions, whereas it becomes smaller for the outer solutions. If the flow is adiabatic, this derivative coincides with $du_{\rm post}(r)/dr$ at the shock radius for the critical luminosity. The neutrino heating, however, makes the former slightly smaller than the latter. This characteristic will be utilized in § 4.

Finally, let us discuss what happens when the luminosity exceeds the critical value. Since there is no steady solution, we should address this issue with time-dependent calculations. However, we can infer at least the initial response of the shock with a simpler analysis. We can see from Figure 1 that when the luminosity exceeds the critical value, the downstream velocity at the shock wave becomes inevitably smaller than $u_{\rm post}(r)$. In addition, the downstream entropy should be larger than that for the critical luminosity, because of the higher luminosity. We can regard this situation as a Riemann problem that has a discontinuity with a velocity slightly lower and an entropy slightly larger in the downstream than those satisfying the Rankine-Hugoniot relations. The solution of the Riemann problem tells us that a shock wave will propagate outward, while a weak rarefaction wave or another weak shock wave will propagate inward at the same time (Courant & Friedrichs 1976); in other words, the shock wave revives. Thus, we can conclude that the condition for the shock to revive is that the neutrino luminosity exceed the critical value.

3. STABILITY AGAINST RADIAL PERTURBATIONS

In the previous section, we found that there are two branches of steady solutions for an accretion flow with a shock. In this section we discuss which type of solutions is realized, examining the stability of these solutions with a global linear analysis. We consider perturbations of the neutrino luminosity; that is, nonadiabatic effects are taken into account.

In this paper, stability only against radial perturbations is considered. This is because we did not take into account the effects of convection in obtaining the unperturbed flows in the previous section. There is, in general, a region where heating prevails over cooling under the irradiation of neutrinos; in this region, entropy increases in the direction of gravity and the flow is convectively unstable. Thus our solutions are convectively unstable against nonradial perturbations, which fact is of no consequence here, though.

Since we consider perturbations accompanying variations of the positions of the inner and outer boundaries, it is convenient to introduce a new variable x, defined as

$$x \equiv (r - r_\nu)/(r_s - r_\nu), \tag{7}$$

where r_s denotes the shock radius. Then, the basic equations describing the time-dependent flows are written as

$$\frac{\partial \rho}{\partial t} - \frac{1}{r_s - r_\nu}\left[x\frac{\partial r_s}{\partial t} + (1-x)\frac{\partial r_\nu}{\partial t}\right]\frac{\partial \rho}{\partial x} + \frac{2\rho u_r}{r} + \frac{\rho}{r_s - r_\nu}\frac{\partial u_r}{\partial x} + \frac{u_r}{r_s - r_\nu}\frac{\partial \rho}{\partial x} = 0, \tag{8}$$

$$\frac{\partial u_r}{\partial t} - \frac{1}{r_s - r_\nu}\left[x\frac{\partial r_s}{\partial t} + (1-x)\frac{\partial r_\nu}{\partial t}\right]\frac{\partial u_r}{\partial x} + \frac{u_r}{r_s - r_\nu}\frac{\partial u_r}{\partial x} + \frac{1}{r_s - r_\nu}\frac{1}{\rho}\frac{\partial p}{\partial x} + \frac{GM}{r^2} = 0, \tag{9}$$

$$\begin{aligned}\frac{\partial \epsilon}{\partial t} &- \frac{1}{r_s - r_\nu}\left[x\frac{\partial r_s}{\partial t} + (1-x)\frac{\partial r_\nu}{\partial t}\right]\frac{\partial \epsilon}{\partial x} - \frac{p}{\rho^2}\frac{\partial \rho}{\partial t} \\ &+ \frac{1}{r_s - r_\nu}\left[x\frac{\partial r_s}{\partial t} + (1-x)\frac{\partial r_\nu}{\partial t}\right]\frac{p}{\rho^2}\frac{\partial \rho}{\partial x} + \frac{u_r}{r_s - r_\nu}\frac{\partial \epsilon}{\partial x} - \frac{u_r}{r_s - r_\nu}\frac{p}{\rho^2}\frac{\partial \rho}{\partial x} - \dot{q} = 0.\end{aligned} \tag{10}$$

Since we assume that the flow outside the shock is steady, the Rankine-Hugoniot relations at the outer boundary are expressed as

$$\rho(u_r - u_s) = \rho_f(u_f - u_s), \qquad \rho(u_r - u_s)^2 + p = \rho_f(u_f - u_s)^2, \qquad \tfrac{1}{2}(u_r - u_s)^2 + \epsilon + p/\rho = \tfrac{1}{2}(u_f - u_s)^2, \tag{11}$$

where u_s is the shock velocity, which can be written as $u_s = \partial r_s/\partial t$. In calculating the perturbations of the heating and cooling rates, we assume, for simplicity, that the effective temperature of the neutrinos is not perturbed.

We perform a linear analysis, assuming that all the perturbed quantities have a time dependence of the form $e^{\omega t}$. In the rest of this section, a subscript 1 is attached to the perturbed quantities and a subscript 0 to the unperturbed ones. Then the equations describing the perturbations become

$$\begin{aligned}&\frac{\partial(\rho_1/\rho_0)}{\partial x} + \frac{\partial(u_{r,1}/u_{r,0})}{\partial x} + \frac{r_{s,0} - r_{\nu,0}}{u_{r,0}}\omega\frac{\rho_1}{\rho_0} + \frac{2}{r_0}\left(r_{s,0}\frac{r_{s,1}}{r_{s,0}} - r_{\nu,0}\frac{r_{\nu,1}}{r_{\nu,0}}\right) + \left(2\frac{r_{s,0} - r_{\nu,0}}{r_0} + \frac{\partial \ln \rho_0}{\partial x} + \frac{\partial \ln u_{r,0}}{\partial x}\right)\left(\frac{\rho_1}{\rho_0} + \frac{u_{r,1}}{u_{r,0}}\right) \\ &\quad + \left(\frac{1}{r_0}\frac{\partial \ln u_{r,0}}{\partial x} + \frac{1}{r_0}\frac{\partial \ln \rho_0}{\partial x} - \frac{\omega}{u_{r,0}}\frac{\partial \ln \rho_0}{\partial x}\right)\left[xr_{s,0}\frac{r_{s,1}}{r_{s,0}} + (1-x)r_{\nu,0}\frac{r_{\nu,1}}{r_{\nu,0}}\right] = 0,\end{aligned} \tag{12}$$

$$\begin{aligned}&\frac{\partial(u_{r,1}/u_{r,0})}{\partial x} + \frac{1}{u_{r,0}^2}\frac{p_{N,0}}{\rho_0}\frac{\partial(\rho_1/\rho_0)}{\partial x} + \frac{1}{u_{r,0}^2}\frac{4p_{R,0} + p_{N,0}}{\rho_0}\frac{\partial(T_1/T_0)}{\partial x} + \left(\frac{r_{s,0} - r_{\nu,0}}{u_{r,0}}\omega + 2\frac{\partial \ln u_{r,0}}{\partial x}\right)\frac{u_{r,1}}{u_{r,0}} \\ &\quad - \frac{1}{u_{r,0}^2}\frac{4p_{R,0}}{\rho_0}\frac{\partial \ln T_0}{\partial x}\frac{\rho_1}{\rho_0} + \left(\frac{1}{u_{r,0}^2}\frac{p_{N,0}}{\rho_0}\frac{\partial \ln \rho_0}{\partial x} + \frac{1}{u_{r,0}^2}\frac{16p_{R,0} + p_{N,0}}{\rho_0}\frac{\partial \ln T_0}{\partial x}\right)\frac{T_1}{T_0} \\ &\quad + \left[\left(\frac{2}{r_0} - \frac{\omega}{u_{r,0}}\right)\frac{\partial \ln u_{r,0}}{\partial x} + \frac{2}{r_0}\frac{1}{u_{r,0}^2}\frac{p_{N,0}}{\rho_0}\frac{\partial \ln \rho_0}{\partial x} + \frac{2}{r_0}\frac{1}{u_{r,0}^2}\frac{4p_{R,0} + p_{N,0}}{\rho_0}\frac{\partial \ln T_0}{\partial x}\right]\left[xr_{s,0}\frac{r_{s,1}}{r_{s,0}} + (1-x)r_{\nu,0}\frac{r_{\nu,1}}{r_{\nu,0}}\right] \\ &\quad + \frac{GM}{r_0^2 u_{r,0}^2}\left(r_{s,0}\frac{r_{s,1}}{r_{s,0}} - r_{\nu,0}\frac{r_{\nu,1}}{r_{\nu,0}}\right) = 0,\end{aligned} \tag{13}$$

$$\begin{aligned}&-\frac{4p_{R,0} + p_{N,0}}{\rho_0}\frac{\partial(\rho_1/\rho_0)}{\partial x} + \frac{12p_{R,0} + (3/2)p_{N,0}}{\rho_0}\frac{\partial(T_1/T_0)}{\partial x} + \left[-\frac{4p_{R,0} + p_{N,0}}{\rho_0}\frac{\partial \ln \rho_0}{\partial x} + \frac{12p_{R,0} + (3/2)p_{N,0}}{\rho_0}\frac{\partial \ln T_0}{\partial x}\right]\frac{u_{r,1}}{u_{r,0}} \\ &\quad + \left[-(r_{s,0} - r_{\nu,0})\frac{4p_{R,0} + p_{N,0}}{\rho_0}\frac{\omega}{u_{r,0}} + \frac{4p_{R,0}}{\rho_0}\frac{\partial \ln \rho_0}{\partial x} - \frac{12p_{R,0}}{\rho_0}\frac{\partial \ln T_0}{\partial x} - \frac{r_{s,0} - r_{\nu,0}}{u_{r,0}}\frac{\partial \dot{q}}{\partial \rho}\rho_0\right]\frac{\rho_1}{\rho_0} \\ &\quad + \left[(r_{s,0} - r_{\nu,0})\frac{12p_{R,0} + (3/2)p_{N,0}}{\rho_0}\frac{\omega}{u_{r,0}} - \frac{16p_{R,0} + p_{N,0}}{\rho_0}\frac{\partial \ln \rho_0}{\partial x} + \frac{48p_{R,0} + (3/2)p_{N,0}}{\rho_0}\frac{\partial \ln T_0}{\partial x} - \frac{r_{s,0} - r_{\nu,0}}{u_{r,0}}\frac{\partial \dot{q}}{\partial T}T_0\right]\frac{T_1}{T_0} \\ &\quad + \left[\frac{4p_{R,0} + p_{N,0}}{\rho_0}\frac{\omega}{u_{r,0}}\frac{\partial \ln \rho_0}{\partial x} - \frac{12p_{R,0} + (3/2)p_{N,0}}{\rho_0}\frac{\omega}{u_{r,0}}\frac{\partial \ln T_0}{\partial x} - \frac{r_{s,0} - r_{\nu,0}}{u_{r,0}}\frac{\partial \dot{q}}{\partial r}\right]\left[xr_{s,0}\frac{r_{s,1}}{r_{s,0}} + (1-x)r_{\nu,0}\frac{r_{\nu,1}}{r_{\nu,0}}\right] \\ &\quad - \frac{\dot{q}}{u_{r,0}}\left(r_{s,0}\frac{r_{s,1}}{r_{s,0}} - r_{\nu,0}\frac{r_{\nu,1}}{r_{\nu,0}}\right) - \frac{r_{s,0} - r_{\nu,0}}{u_{r,0}}\frac{\partial \dot{q}}{\partial L_{\nu_e}}L_{\nu_e,0}\frac{L_{\nu_e,1}}{L_{\nu_e,0}} - \frac{r_{s,0} - r_{\nu,0}}{u_{r,0}}\frac{\partial \dot{q}}{\partial r_\nu}r_{\nu,0}\frac{r_{\nu,1}}{r_{\nu,0}} = 0,\end{aligned} \tag{14}$$

where $p_{R,0}$, $p_{N,0}$, and r_0 are defined as

$$p_{R,0} \equiv \frac{11\pi^2}{180}\frac{k^4}{c^3\hbar^3}T_0^4, \qquad p_{N,0} \equiv \rho_0 k T_0/m_N, \qquad r_0 \equiv xr_{s,0} + (1-x)r_{\nu,0}. \tag{15}$$

All the variables, $u_{r,1}/u_{r,0}$, ρ_1/ρ_0, T_1/T_0, $r_{s,1}/r_{s,0}$, $r_{\nu,1}/r_{\nu,0}$, and $L_{\nu_e,1}/L_{\nu_e,0}$, and the eigenvalue ω can be complex-valued.

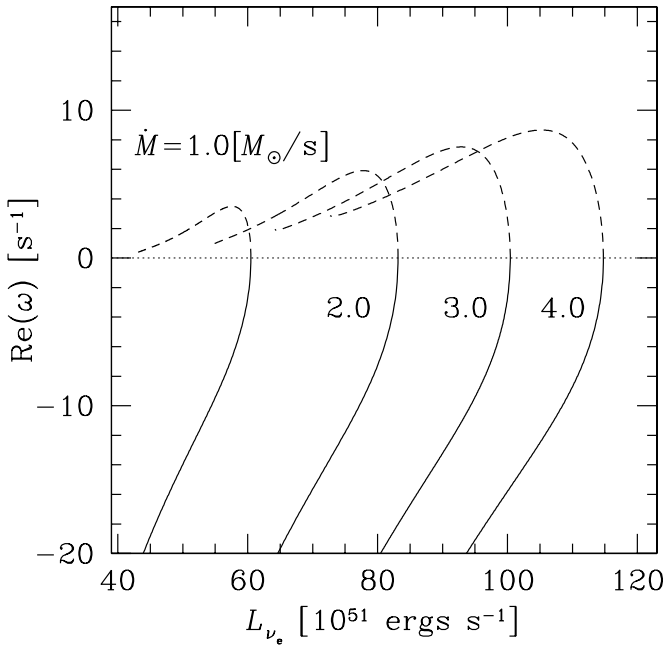

FIG. 3.—Same as Fig. 2, but for the growth rates under radial perturbations.

The outer boundary conditions ($x = 1$) become

$$\left(\frac{2}{r_{s,0}^2}\frac{\rho_{f,0}}{\rho_0}\frac{u_{f,0}}{u_{r,0}} + \frac{\omega}{r_{s,0}^{1/2}}\frac{\rho_{f,0}}{\rho_0} - \rho_0\omega r_{s,0}\right)\frac{r_{s,1}}{r_{s,0}} + \rho_0 u_{r,0}\left(\frac{u_{r,1}}{u_{r,0}} + \frac{\rho_1}{\rho_0}\right) = 0, \tag{16}$$

$$\left(\frac{5}{2r_{s,0}^{5/2}}\frac{\rho_{f,0}}{\rho_0}\frac{u_{f,0}^2}{u_{r,0}^2} + \frac{2\omega}{r_{s,0}}\frac{\rho_{f,0}}{\rho_0}\frac{u_{f,0}}{u_{r,0}} - 2\omega r_{s,0}\rho_0 u_{r,0}\right)\frac{r_{s,1}}{r_{s,0}} + 2\rho_0 u_{r,0}^2\frac{u_{r,1}}{u_{r,0}} + (\rho_0 u_{r,0}^2 + p_{N,0})\frac{\rho_1}{\rho_0} + (4p_{R,0} + p_{N,0})\frac{T_1}{T_0} = 0, \tag{17}$$

$$\left(\frac{1}{2r_{s,0}}\frac{u_{f,0}^2}{u_{r,0}^2} - \omega r_{s,0}^{1/2}\frac{u_{f,0}}{u_{r,0}} - \omega r_{s,0}u_{r,0}\right)\frac{r_{s,1}}{r_{s,0}} + u_{r,0}^2\frac{u_{r,1}}{u_{r,0}} - 4\frac{p_{R,0}}{\rho_0}\frac{\rho_1}{\rho_0} + \frac{16p_{R,0} + (5/2)p_{N,0}}{\rho_0}\frac{T_1}{T_0} = 0, \tag{18}$$

where $\rho_{f,0}$ and $u_{f,0}$ are the density and velocity of the free fall at the shock in the unperturbed state. Since we set the neutrinosphere as the inner boundary ($x = 0$) and the density is fixed there by definition, we impose the condition

$$\rho_1/\rho_0 = 0 \tag{19}$$

at the inner boundary. In addition, we assume

$$u_{r,1}/u_{r,0} = 0 \tag{20}$$

at the inner boundary, supposing that the infalling matter comes to rest on the neutron star. Since the neutrino temperature is assumed to be unperturbed, the variation of the luminosity is related to that of the neutrinosphere radius as

$$\frac{L_{\nu_e,1}}{L_{\nu_e,0}} = 2\frac{r_{\nu,1}}{r_{\nu,0}}. \tag{21}$$

The above equations are solved as follows: We first take trial values of ω and $r_{\nu,1}/r_{\nu,0}$ ($r_{s,1}/r_{s,0}$ is set to unity) and solve the outer boundary conditions (eqs. [16]–[18]) and equations (12)–(14) from the outer boundary to the inner boundary. The solution obtained in this way does not, in general, meet the inner boundary conditions (eqs. [19]–[20]). We then improve the values of ω and $r_{\nu,1}/r_{\nu,0}$ and repeat the procedure until equations (19) and (20) are satisfied at the inner boundary.

We find, for a given unperturbed solution, many modes with complex eigenvalues (probably an infinite number of overtones, in fact) and only one mode with a real eigenvalue. All modes with complex eigenvalues are damped, namely, the real part of the eigenvalue is negative, owing to the thermal-smearing effect of the neutrino irradiation. We display only the results for the mode with a real eigenvalue. The growth rates are shown in Figure 3. One can see that the inner solutions are always stable, while the outer solutions are always unstable. Further, when the luminosity reaches the critical value, both solutions become neutral. The eigenfunctions are shown in Figure 4. Ratios of the luminosity perturbation to that of the shock radius are shown in Figure 5. Since the amplitude of

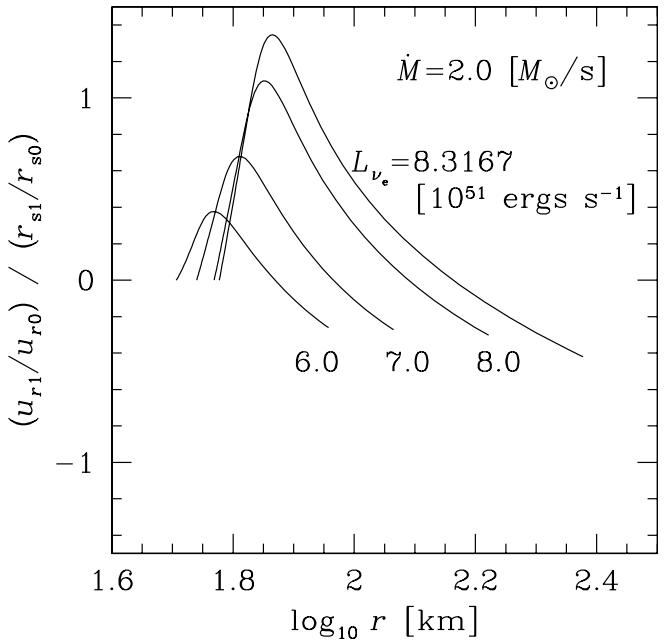

FIG. 4*a*

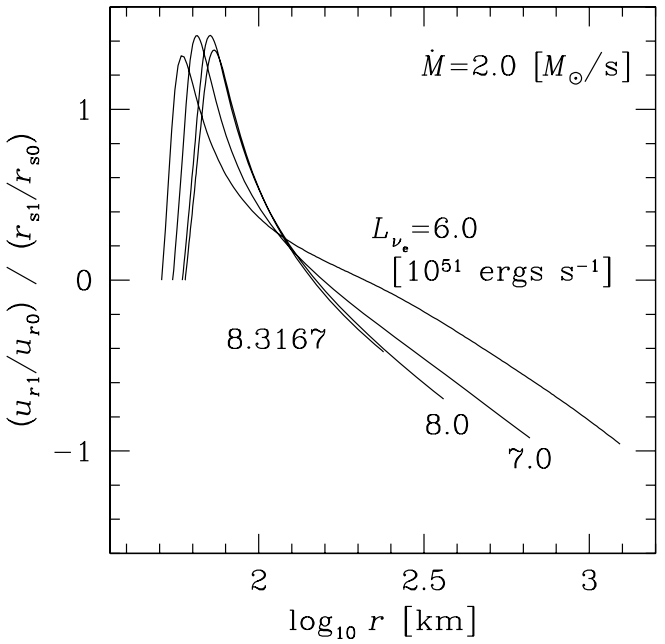

FIG. 4*b*

FIG. 4.—Eigenfunctions of radial perturbations with $\dot{M} = 2.0\ M_\odot\ \mathrm{s}^{-1}$ and $L_{\nu_e} = (6, 7, 8) \times 10^{52}$ and 8.3167×10^{52} ergs s^{-1} (the critical value) for (*a*) the inner solutions, from left to right, and (*b*) the outer solutions, from right to left near the shock. Note that the functions are defined in different radial ranges for different models.

the luminosity perturbations is twice that of the neutrinosphere radius, we can see that the perturbations of the inner and outer boundaries are in phase for the inner solutions, whereas they have opposite phase for the outer solutions.

We should note again that we have investigated stability against radial perturbations only. As several authors have pointed out, spherical accretion shocks are, in general, unstable against nonradial perturbations (Houck & Chevalier 1992; Foglizzo 2002; Blondin et al. 2003). In this sense, we cannot say that the inner solutions are stable. Detailed studies of the stability against nonradial perturbations will be necessary with the effects of convection and neutrino irradiation properly taken into account.

4. EFFECTS OF ROTATION

In this section, we discuss the effects of rotation on the revival of the shock. We extend the one-dimensional analysis of § 2 to the two-dimensional case. A brief summary of our results in this section has appeared previously (Yamada et al. 2004). Since, as we found in the previous section, the outer solutions are unstable, we consider only the inner solutions in this section. The assumptions and simplifications mentioned in § 2 are also adopted here, except for the assumptions about the flows outside the shock, which will be

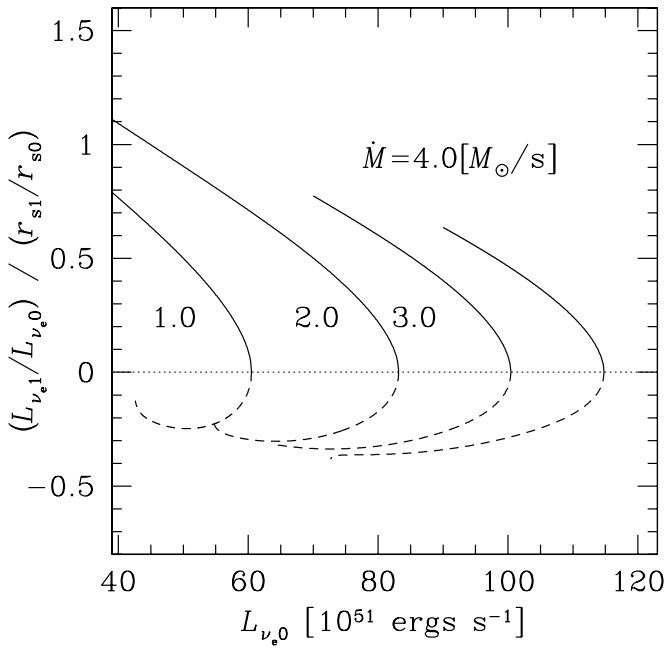

FIG. 5.—Same as Fig. 2, but for the ratio of luminosity perturbation to that of shock radius.

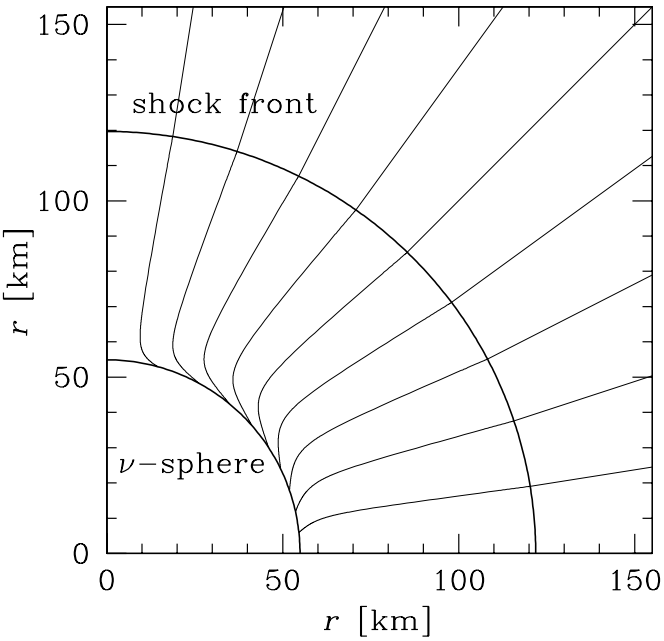

FIG. 6.—Meridian section of a collapsing star and stream curves for $\dot{M} = 2.0\ M_\odot\ \mathrm{s}^{-1}$, $L_{\nu_e} = 7 \times 10^{52}$ ergs s^{-1}, and a rotational frequency of 0.1 s^{-1} at $r = 1000$ km.

addressed below. Assuming axial symmetry, we use spherical coordinates. Then the basic equations describing the steady flow inside the shock are written as

$$\frac{1}{r^2}\frac{\partial}{\partial r}(r^2\rho u_r) + \frac{1}{r\sin\theta}\frac{\partial}{\partial\theta}(\sin\theta\rho u_\theta) = 0, \qquad u_r\frac{\partial u_r}{\partial r} + \frac{u_\theta}{r}\frac{\partial u_r}{\partial\theta} - \frac{u_\theta^2 + u_\phi^2}{r} = -\frac{1}{\rho}\frac{\partial p}{\partial r} - \frac{GM}{r^2}, \tag{22}$$

$$u_r\frac{\partial u_\theta}{\partial r} + \frac{u_\theta}{r}\frac{\partial u_\theta}{\partial\theta} + \frac{u_r u_\theta}{r} - \frac{u_\phi^2\cot\theta}{r} = -\frac{1}{\rho r}\frac{\partial p}{\partial\theta}, \qquad u_r\frac{\partial u_\phi}{\partial r} + \frac{u_\theta}{r}\frac{\partial u_\phi}{\partial\theta} + \frac{u_\phi u_r}{r} + \frac{u_\theta u_\phi\cot\theta}{r} = 0, \tag{23}$$

$$u_r\left(\frac{\partial\epsilon}{\partial r} - \frac{p}{\rho^2}\frac{\partial\rho}{\partial r}\right) + \frac{u_\theta}{r}\left(\frac{\partial\epsilon}{\partial\theta} - \frac{p}{\rho^2}\frac{\partial\rho}{\partial\theta}\right) = \dot{q}, \tag{24}$$

where $\boldsymbol{u}$ denotes the velocity and the other notation is the same as in § 2.

Since we seek solutions with axial and equatorial symmetry, we impose the following conditions:

$$u_\phi = u_\theta = \frac{\partial u_r}{\partial\theta} = \frac{\partial\rho}{\partial\theta} = \frac{\partial T}{\partial\theta} = 0 \quad \text{at} \quad \theta = 0, \qquad u_\theta = \frac{\partial u_r}{\partial\theta} = \frac{\partial u_\phi}{\partial\theta} = \frac{\partial\rho}{\partial\theta} = \frac{\partial T}{\partial\theta} = 0 \quad \text{at} \quad \theta = \frac{\pi}{2}. \tag{25}$$

The outer and inner boundaries are set at the shock surface and neutrinosphere, respectively. The neutrinosphere will be oblate because of centrifugal force, and as a result, the neutrino flux will be anisotropic (Kotake et al. 2003). Such an effect may have some influence on the explosion (Shimizu et al. 2001). Since our concern here is the hydrodynamic effect of rotation on the accretion flow, we assume that the neutrinosphere is spherical and that the neutrino flux and temperature are isotropic. Unlike in § 2, the shock surface is not spherical and is oblique to the flow, in general.

As in the one-dimensional calculations, we impose the condition that the density is 10^{11} g cm^{-3} at the inner boundary. The Rankine-Hugoniot relations for oblique shocks are imposed at the outer boundary. For the flows outside the shock, we make the following approximations:

1. The flows are radial except for rotation and free fall.
2. The density is independent of latitude, and thus the accretion is isotropic outside the shock.
3. The rotational frequency is independent of latitude and the specific angular momentum is conserved along each stream curve.

Although these assumptions are artificial and not self-consistent, in reality, since the centrifugal force is small compared with the gravity or the inertia, the radial component of the velocity must be predominant.

We define the parameter f as the rotational frequency at a radius of 1000 km. We performed the calculations for $f = 0.03$ s^{-1} and $f = 0.1$ s^{-1}, which correspond to specific angular momenta averaged over the whole sphere outside the shock wave surface of 1.256×10^{15} and 4.187×10^{15} cm^2 s^{-1}, respectively. (The definition of the specific angular momentum is that employed by Heger et al. [2000, 2004] in their calculations of stellar evolution.)

In Figure 6, we show the stream curves for the parameter values $\dot{M} = 2.0\ M_\odot\ \mathrm{s}^{-1}$, $L_{\nu_e} = 7.0 \times 10^{52}$ ergs s^{-1}, and $f = 0.1$ s^{-1}. We can see that the flow is pushed toward the equatorial plane as a result of centrifugal force. The stream curves bend rather abruptly near

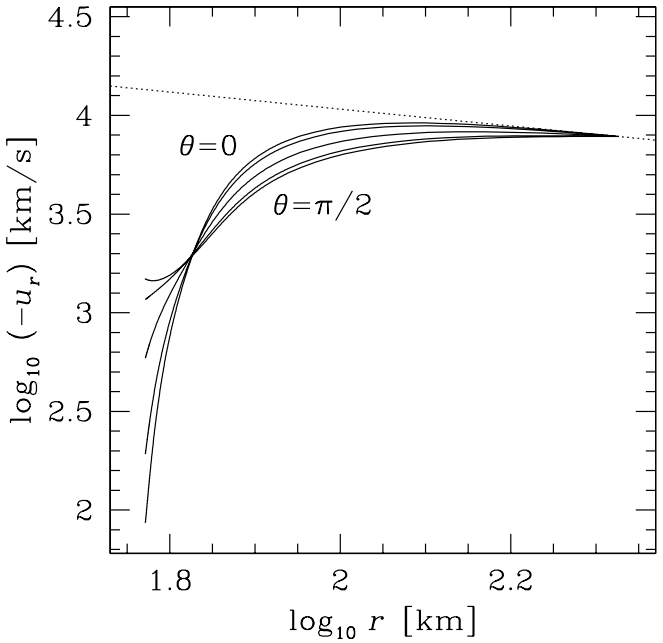

FIG. 7.—Radial velocity at latitudes θ of 0, $\pi/8$, $\pi/4$, $3\pi/8$, and $\pi/2$ for the rotating steady accretion flow with $\dot{M} = 2.0\,M_\odot\,\mathrm{s}^{-1}$, $L_{\nu_e} = 8.10 \times 10^{52}$ ergs s^{-1} (the critical value), and rotational frequency 0.1 s^{-1} at $r = 1000$ km, from top to bottom. The dotted line shows the downstream value satisfying the Rankine-Hugoniot relations at each radius.

the neutrinosphere because the infalling matter is decelerated as it lands on the neutron star's surface and the radial velocity falls rapidly there. We also note that the shock surface is slightly deformed into an oblate configuration, and the flows are directed toward the rotation axis at large radii.

The angular dependence of the radial velocity inside the shock is shown in Figure 7. At large radii, the velocity is larger near the rotation axis than at the equatorial plane, whereas the opposite is true near the inner boundary. We attribute this behavior to the variation of the cross section of the flow. The theory of Laval nozzles tells us that subsonic flows are decelerated when the cross section of the nozzle gets larger, and vice versa (Landau & Lifshitz 1987). As we saw in Figure 6, the flow is bent toward the equatorial plane near the neutrinosphere but toward the rotation axis near the shock. As a result, at small radii the cross section of the flow becomes larger near the axis, whereas it gets smaller near the equatorial plane, and vice versa at large radii. Thus we obtain the observed angular dependence of the velocity.

Next we discuss the effect of rotation on the critical luminosity. In Figure 8, we show the dependence of the critical luminosity on the mass accretion rate. One can see that the smaller the mass accretion rate is, or the larger the rotational frequency is, the more

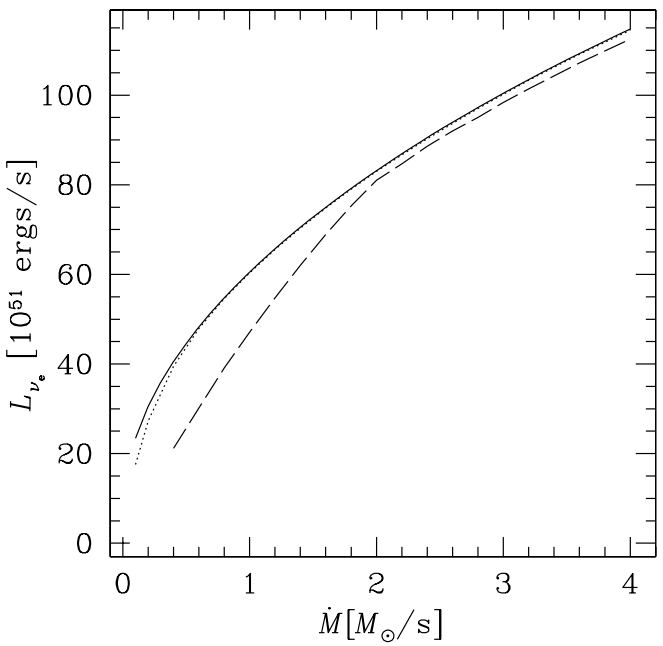

FIG. 8.—Critical luminosity. The solid curve denotes the spherically symmetric case, and the others correspond to the rotational models. The rotational frequencies are 0.03 and 0.1 s^{-1} at 1000 km for the dotted and dashed curves, respectively. No steady solution exists for luminosities above the critical value.

reduced the critical luminosity is. According to the results of our calculations, if f is 0.03 s^{-1} and the accretion rate is 0.1 $M_\odot$ s^{-1}, the critical value is about 25% smaller than that of a spherically symmetric flow with the same mass accretion rate. If the rotation parameter is 0.1 s^{-1}, the effect is more remarkable. For mass accretion rates of 1.0 and 0.5 $M_\odot$ s^{-1}, we obtain critical luminosities reduced by about 25% and 43%, respectively, from the value for a spherically symmetric flow.

Finally, we discuss the fate of the shock wave when the critical luminosity is reached. In § 2 we discussed the movement of the steady shock for the inner solutions; the radial derivative of the infall velocity increases when the neutrino luminosity is raised, and it becomes nearly equal to that of $u_{\rm post}(r)$ when the luminosity reaches the critical value. The angular dependence of the velocity at the critical luminosity is shown in Figure 7. One can see that the derivative is largest at $\theta = 0$. This suggests that the steady flow first ceases to exist at the axis. Thus, we can infer that the stalled shock is revived and starts to propagate outward first at the rotation axis and that the jetlike explosion follows, although time-dependent numerical simulations are necessary to confirm this.

This breakup of the shock at the rotation axis and the resulting reduction of the critical luminosity are also attributable to changes of radial flow velocities, which can be understood based on the theory of Laval nozzles, as we saw above. The variation of flow cross section causes an acceleration of the radial flow at large radii near the rotation axis, whereas it leads to a deceleration near the equatorial plane. As a result, the revival of the stalled shock is more easily attained at the rotation axis for lower neutrino luminosities than in the case of a spherically symmetric flow.

5. SUMMARY AND DISCUSSION

In this paper, we have investigated the behavior of the stalled shock in a supernova's core and the effects of rotation on its revival. Spherically symmetric accretion flows were considered first. We found that there exist two branches of solutions when the luminosity of the irradiating neutrinos is below a critical value. No steady solution exists when the luminosity is higher than the critical value.

In order to consider which of the two solutions is realized below the critical luminosity, we then examined the stability of the spherical accretion flows against radial perturbations and found that the inner solutions are stable while the outer solutions are unstable. In fact, for the small luminosities expected for the early phase of the shock's stagnation, the radii of the outer solutions are extremely large (Fig. 2). Thus, the outer solutions will not occur in reality. The inner solutions are always stable until the neutrino luminosity reaches the critical value, where the two branches merge and the solution becomes neutrally stable. It should be noted, however, that the stability of the outer solutions may be affected by rotation, which we will take up in a future work.

We did not discuss stability against nonradial perturbations, since our models are convectively unstable. Several authors have shown that a spherical accretion shock is unstable against nonradial perturbations. Blondin et al. (2003) demonstrated such an instability for adiabatic perturbations with numerical simulations. Houck & Chevalier (1992) also examined the subject, taking into account cooling processes whose rates are determined locally. In the present situation, however, the heating rates are not determined locally because the flow is irradiated by neutrinos coming out of the proto–neutron star; the perturbations of the flow affect the neutrino luminosity, and the latter then affects the former, by varying the heating and cooling rates. Thus, the problem is different from those just mentioned. A detailed analysis of this situation is left to future work. Furthermore, a stability analysis with rotation taken into account is also an interesting issue.

Finally, we discussed the effects of rotation on the revival of the stalled shock. We showed that rotation lowers the critical luminosity. However, we also claimed that the shock revival would first take place at the rotation axis. We took rotational frequencies of 0.03 and 0.1 s^{-1} at a radius of 1000 km and found that the effect of rotation is substantial. The rotational frequency of newly born neutron stars guessed from the spin-down rate of young pulsars is several tens of rotations per second (Kaspi et al. 1994; van der Swaluw & Wu 2001). Thus, the frequency we adopted here is an order of magnitude higher than the value inferred from observations of young pulsars. It might be possible, however, for this discrepancy to be removed by some mechanism such as magnetic braking in the late phase of the explosion, which could take away the excess angular momentum from the proto–neutron star. In fact, the values we adopted are consistent with those obtained in calculations of the evolution of rotating stars (Heger et al. 2004). In any event, the angular momentum distribution inside massive stars is not yet well understood, because of our poor knowledge of the mechanism of angular momentum transfer (see Heger et al. 2000, 2004). As long as the angular momentum of the infalling matter is large enough, our results suggest that rotation assists the revival of the shock.

In this paper, we have employed various assumptions and simplifications in the formulations. We assumed that the neutrinosphere is spherical and the neutrino flux is isotropic. If the collapsing star is rotating, the proto–neutron star will have angular momentum. Kotake et al. (2003) investigated how the neutrinosphere is affected by rotation. They showed that the neutron star becomes oblate and that, as a result, the emerging flux is more concentrated to the rotation axis. On the other hand, Shimizu et al. (2001) studied how the explosion is affected when the neutrino flux is greater near the rotation axis and claimed that such a neutrino anisotropy can trigger a jetlike explosion in otherwise failed models. Such effects were neglected in this paper only for simplicity and are expected to further reduce the critical luminosity, an expectation we will study in the future.

Convection should also be affected by rotation. Fryer & Heger (2000) have studied such effects with numerical simulations. They found that the centrifugal force reduces the effective gravity and that the efficiency of convection is thus lowered near the equatorial plane. As a result, the explosion energy was also decreased. The explosion, however, becames jetlike. In order to investigate the effect of convection in time-independent models, it is necessary to introduce some simplification, such as mixing-length theory or another formulation to smooth the entropy gradient. This is currently being undertaken.

Finally, the collapsing stars may have magnetic fields, which would be be amplified by rotation. Recent work suggests that the magnetic fields are amplified by differential rotation or magnetorotational instability (Akiyama et al. 2003; Kotake et al. 2004; Ardeljan et al. 2004). If the magnetic energy is amplified to a level comparable to the rotational energy, it must affect the accretion flow and the behavior of the stalled shock as suggested by such work. This issue is also a future task.

This work was partially supported by Grants-in-Aid for the 21st Century Center of Excellence program "Holistic Research and Education Center for Physics of Self-organizing Systems" of Waseda University and for Scientific Research (Nos. 14740166, 14079202) from the Ministry of Education, Science, Sports, and Culture of Japan.

REFERENCES

Akiyama, S., Wheeler, J. C., Meier, D. L., & Lichtenstadt, I. 2003, ApJ, 584, 954
Ardeljan, N. V., Bisnovatyi-Kogan, G. S., & Moiseenko, S. G. 2004, MNRAS, submitted (astro-ph/0410234)
Blondin, J. M., Mezzacappa, A., & DeMarino, C. 2003, ApJ, 584, 971
Buras, R., Rampp, M., Janka, H.-T., & Kifonidis, K. 2003, Phys. Rev. Lett., 90, No. 241101
Burrows, A., & Goshy, J. 1993, ApJ, 416, L75
Courant, R., & Friedrichs, K. O. 1976, Supersonic Flow and Shock Waves (repr.; New York: Springer)
Foglizzo, T. 2002, A&A, 392, 353
Fryer, C. L., & Heger, A. 2000, ApJ, 541, 1033
Heger, A., Langer, N., & Woosley, S. E. 2000, ApJ, 528, 368
Heger, A., Woosley, S. E., Langer, N., & Spruit, H. C. 2004, in IAU Symp. 215, Stellar Rotation, ed. A. Maeder & P. R. J. Eenens (San Francisco: ASP), 591
Herant, M., Benz, W., & Colgate, S. 1992, ApJ, 395, 642
Houck, J. C., & Chevalier, R. A. 1992, ApJ, 395, 592
Janka, H.-T. 2001, A&A, 368, 527
Janka, H.-T., & Müller, E. 1996, A&A, 306, 167
Kaspi, V. M., Manchester, R. N., Siegman, B., Johnston, S., & Lyne, A. G. 1994, ApJ, 422, L83
Kotake, K., Sawai, H., Yamada, S., & Sato, K. 2004, ApJ, 608, 391
Kotake, K., Yamada, S., & Sato, K. 2003, ApJ, 595, 304
Kulkarni, S. R. 1992, Philos. Trans. R. Soc. London A, 341, 77
Landau, L. D., & Lifshitz, E. M. 1987, Fluid Mechanics (2nd rev. ed.; Oxford: Pergamon)
Leonard, D. C., Filippenko, A. V., Barth, A. J., & Matheson, T. 2000, ApJ, 536, 239
Liebendörfer, M., Mezzacappa, A., Thielemann, F.-K., Messer, O. E. B., Hix, W. R., & Bruenn, S. W. 2001, Phys. Rev. D, 63, No. 103004
Liebendörfer, M., Rampp, M., Janka, H.-T., & Mezzacappa, A. 2005, ApJ, 620, 840
Mönchmeyer, R. M., & Müller, E. 1989, in Timing Neutron Stars, ed. H. Ögelman & E. P. J. van den Heuvel (NATO ASI Ser. C, 262) (Dordrecht: Kluwer), 549
Müller, E., Rampp, M., Buras, R., Janka, H.-T., & Shoemaker, D. H. 2004, ApJ, 603, 221
Shapiro, S. L., & Teukolsky, S. A. 1983, in Black Holes, White Dwarfs, and Neutron Stars (New York: Wiley)
Shimizu, T. M., Ebisuzaki, T., Sato, K., & Yamada, S. 2001, ApJ, 552, 756
Spruit, H. C. 2002, A&A, 381, 923
Thompson, T. A., Burrows, A., & Pinto, P. A. 2003, ApJ, 592, 434
van der Swaluw, E., & Wu, Y. 2001, ApJ, 555, L49
Wang, L., et al. 2002, ApJ, 579, 671
Wheeler, J. C. 2003, Am. J. Phys., 71, 11
Wilson, J. R. 1985, in Numerical Astrophysics, ed. J. M. Centrella, J. M. LeBlanc, & R. L. Bowers (Boston: Jones and Bartlett), 422
Yamada, S., Kotake, K., & Yamasaki, T. 2004, New J. Phys., 6, No. 79
Yamada, S., & Sato, K. 1994, ApJ, 434, 268